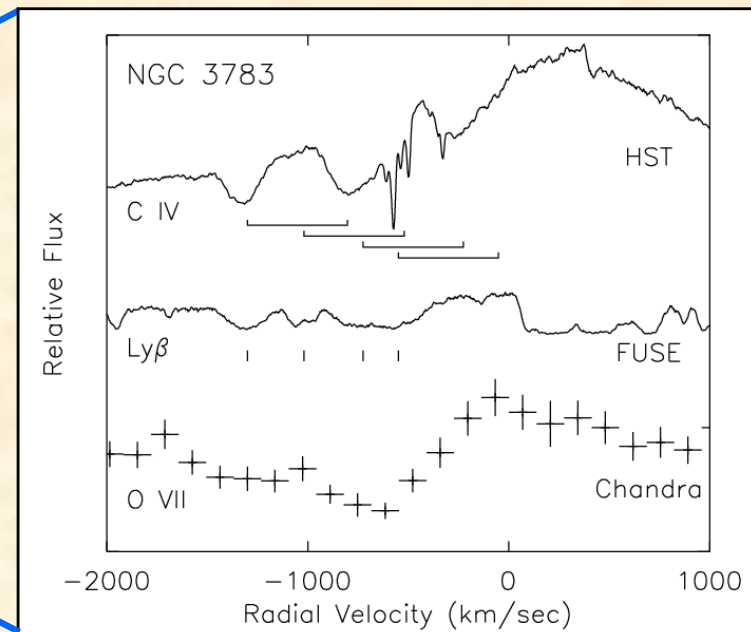
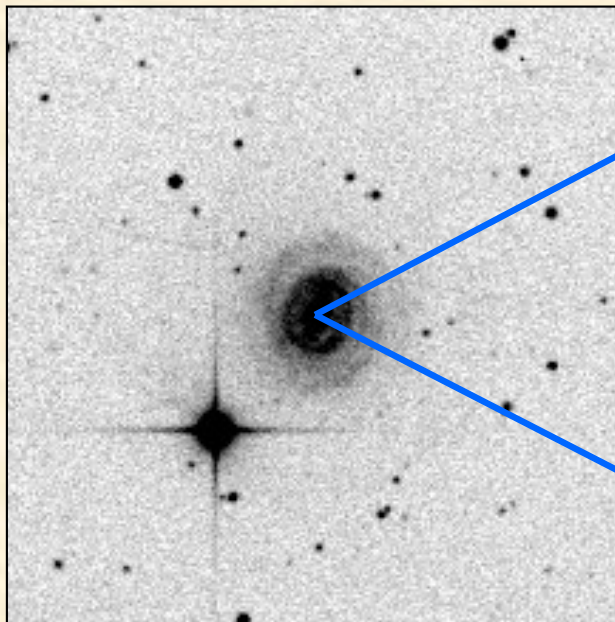


AGN Kinematics

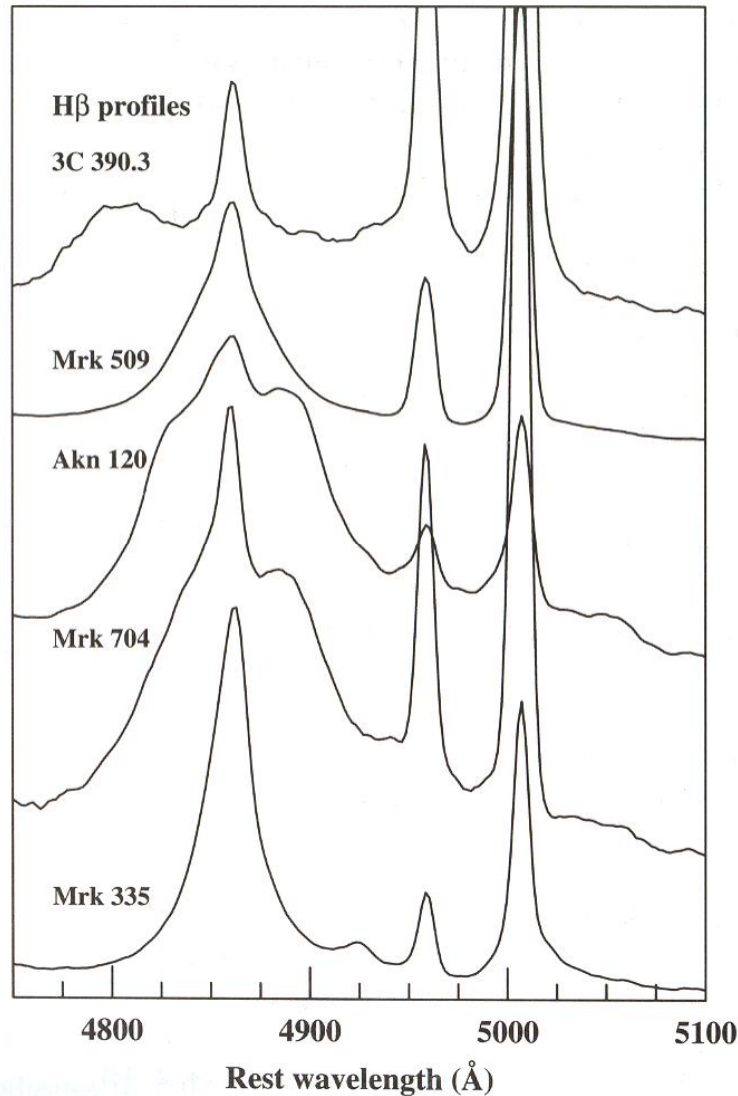
- BLR profiles and kinematics
- Outflows seen in Absorption (AGN Winds)
- Emission-Line Outflows in the NLR



BLR Profiles and Kinematics

BLRG

Sey 1



- Wide variety, many with bumps
- Many BLRGs have double-peaked profiles (after subtraction of NLR)
- Wings are logarithmic, but many kinematic models can reproduce them (Capriotti, et al. 1990, ApJ, 241, 903)

What is the BLR?

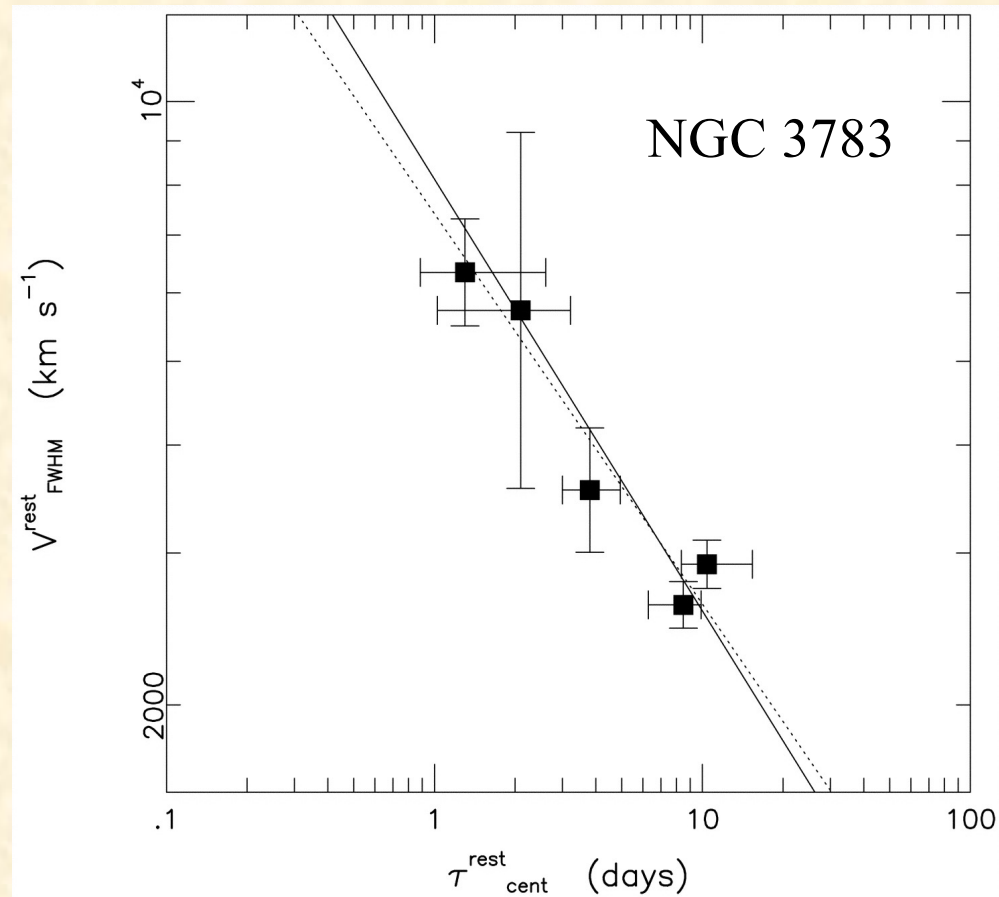
- bloated (irradiated) stars?
- surface of accretion disk?
- clouds in an outflowing wind?

Need more information on, size, geometry, and kinematics

→ Use variability and reverberation mapping

(Peterson, p. 69)

Lags for Different Emission Lines



(Onken & Peterson, 2002, ApJ, 572, 746)

$$\text{FWHM} \sim r^{-0.5}$$

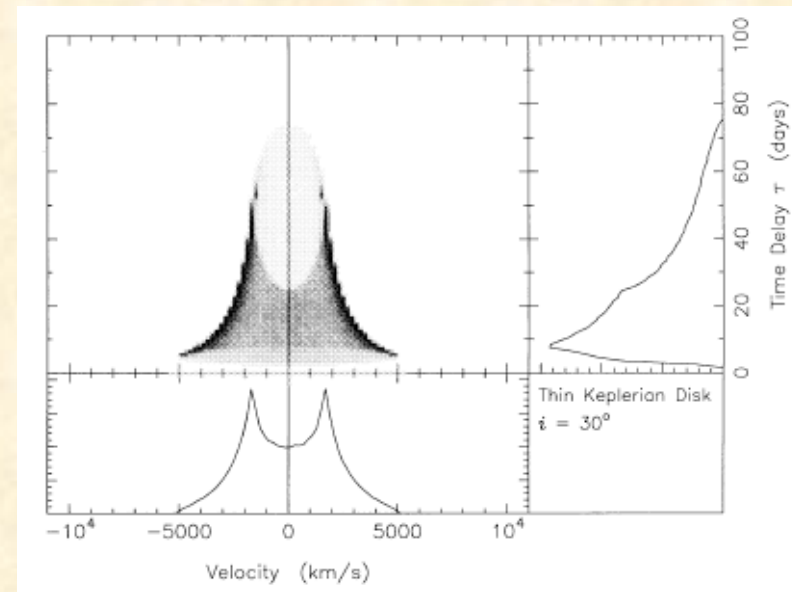
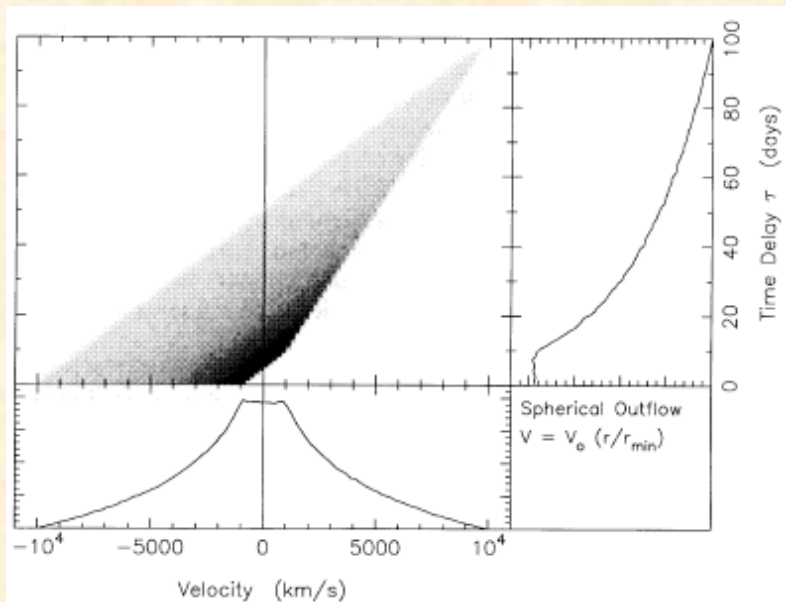
- Suggests gravitational motion (or at least $1/r^2$ force)
- But radiation pressure could be important (Marconi et al. 2008)

Determining the kinematics directly \rightarrow (Radial) velocity-dependent Ψ

$$L(v,t) = \int_{-\infty}^{\infty} \Psi(v,t) C(t-\tau) d\tau,$$

where $L(v,t)$ is the velocity-dependent profile

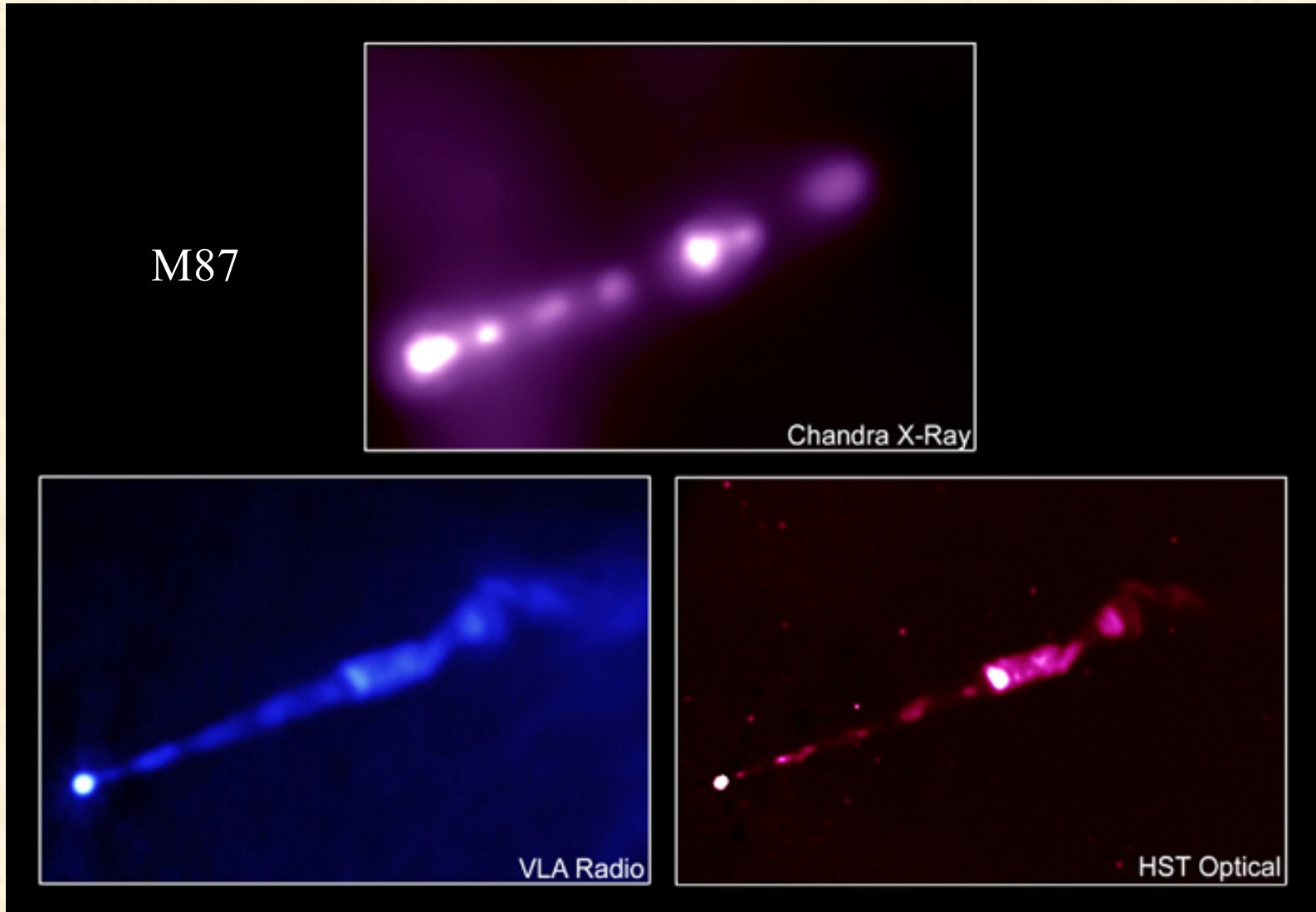
Examples of model $\Psi(v,\tau)$ (Welsh & Horne, 1991, ApJ, 379, 586):



- Determine $\Psi(v,\tau)$ observationally and compare with models
- Recent results (also from forward-modeling simulations) indicate BLR is likely an accretion-disk wind.

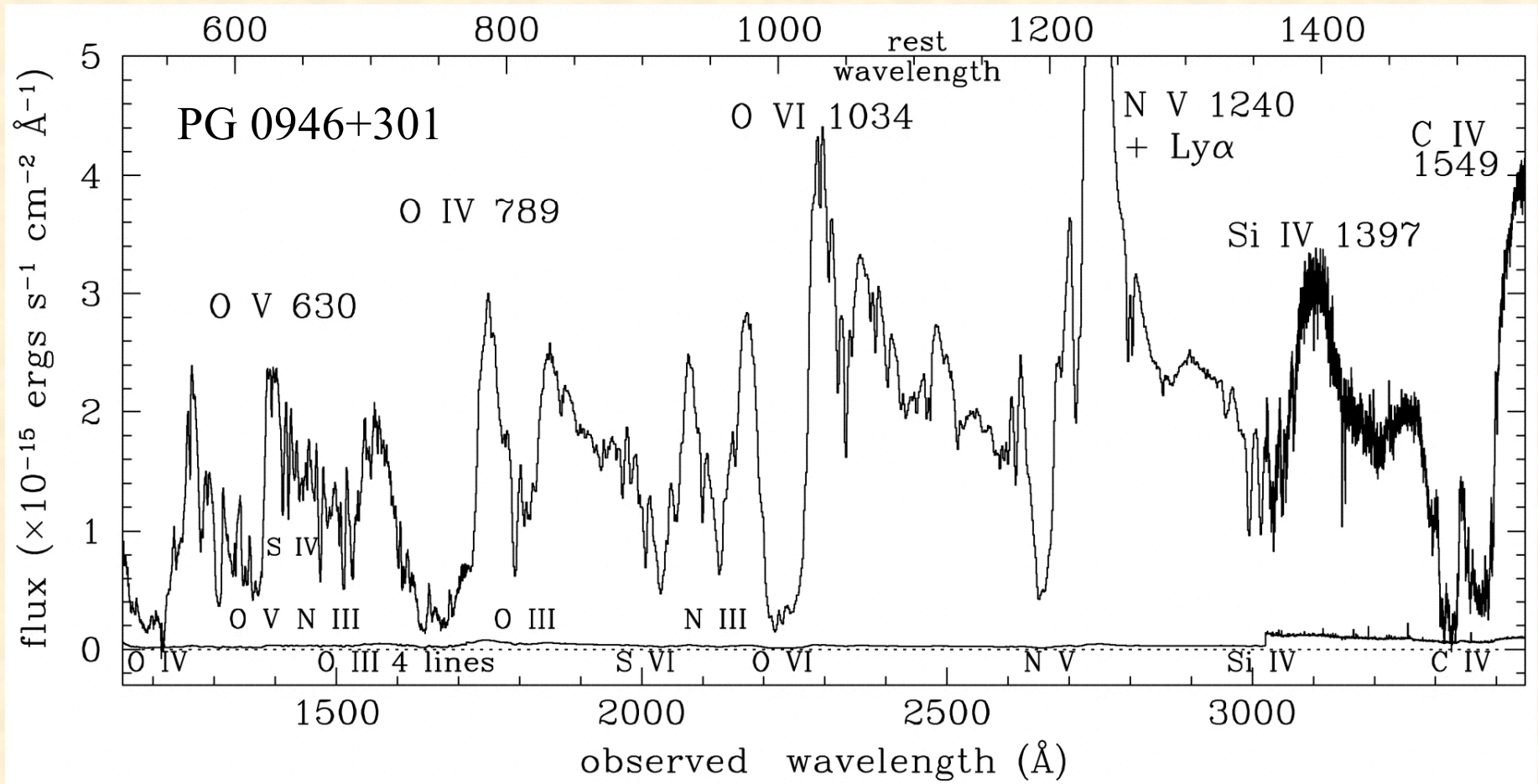
Outflows in AGN: Types

1) Jets in Radio-Loud Galaxies and Quasars



- Highly collimated, low density plasma traveling at relativistic speeds

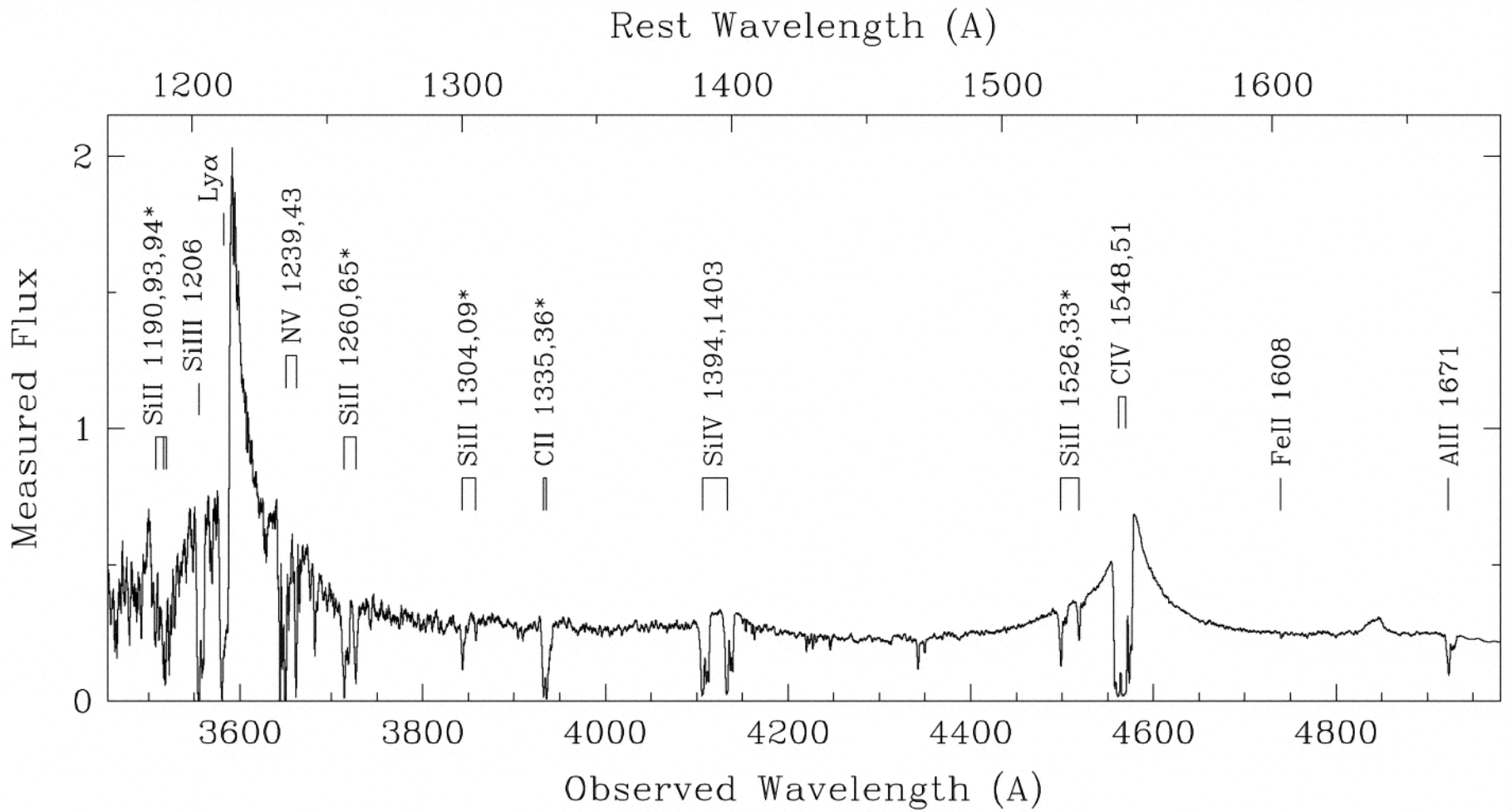
2) Broad Absorption-Line (BAL) Quasars



(Arav et al. 2001, ApJ, 561, 118)

- **Blueshifted** absorption troughs extending up to $\sim 0.2c$
- Observed in $\sim 10\%$ of radio-quiet quasars
- Possibly occur in most quasars, covering $\sim 10\%$ of the AGN sky

3) Quasar “Associated Absorption”

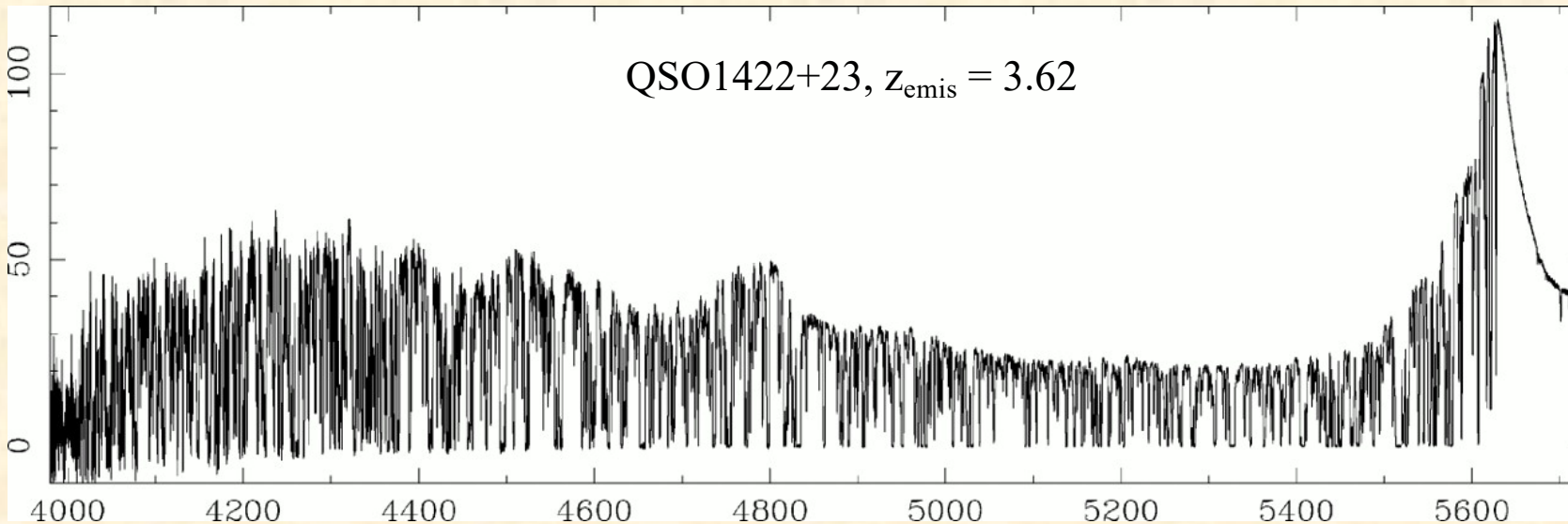


(Hamann et al. 2001, ApJ, 550, 152)

- Discovered as excess absorption lines near z of quasar ($z_{\text{abs}} \approx z_{\text{emis}}$)
- Narrow absorption (FWHM $< 300 \text{ km s}^{-1}$) within 5000 km s^{-1} of z_{emis}
- Mostly blueshifted, which indicates outflow from nucleus

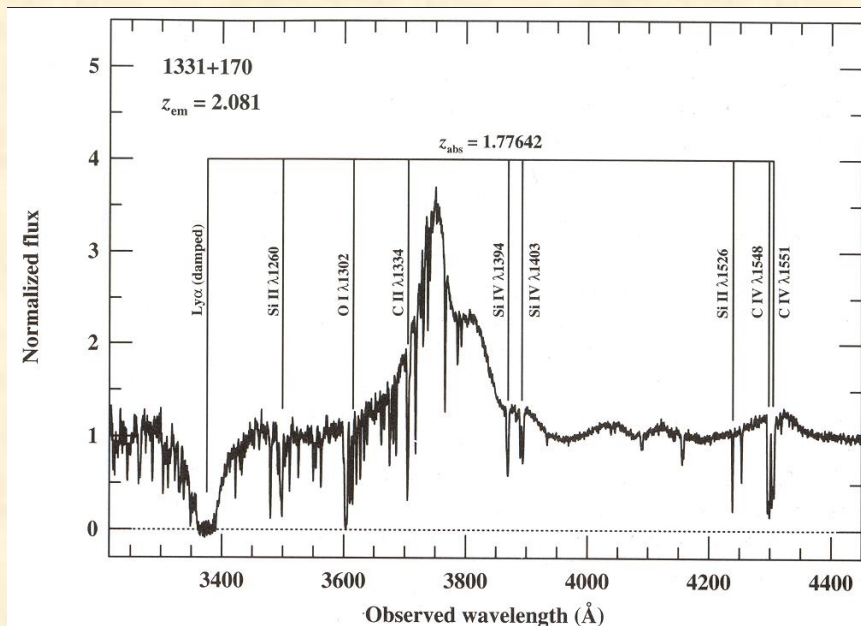
Not to be confused with absorption at $z_{\text{abs}} \ll z_{\text{emis}}$:

a) Ly α Forest - intervening clouds in the intergalactic medium



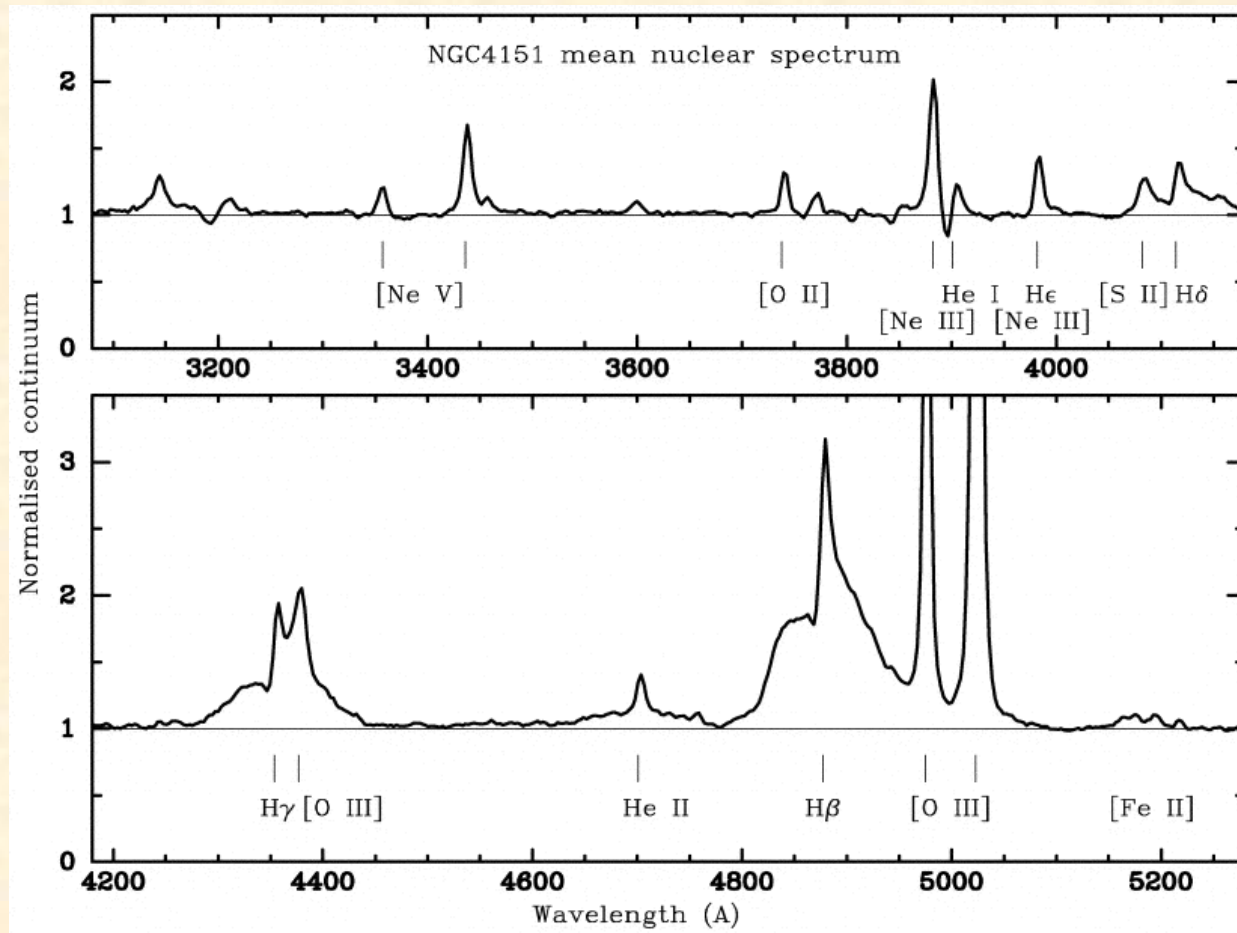
(Rauch, 1998, ARAA, 36, 267)

b) “Metal-line” systems - intervening galaxies and their halos



(Peterson, 1997, An Introduction to AGN, p. 201)

4) “Intrinsic Absorption” in Seyfert Galaxies



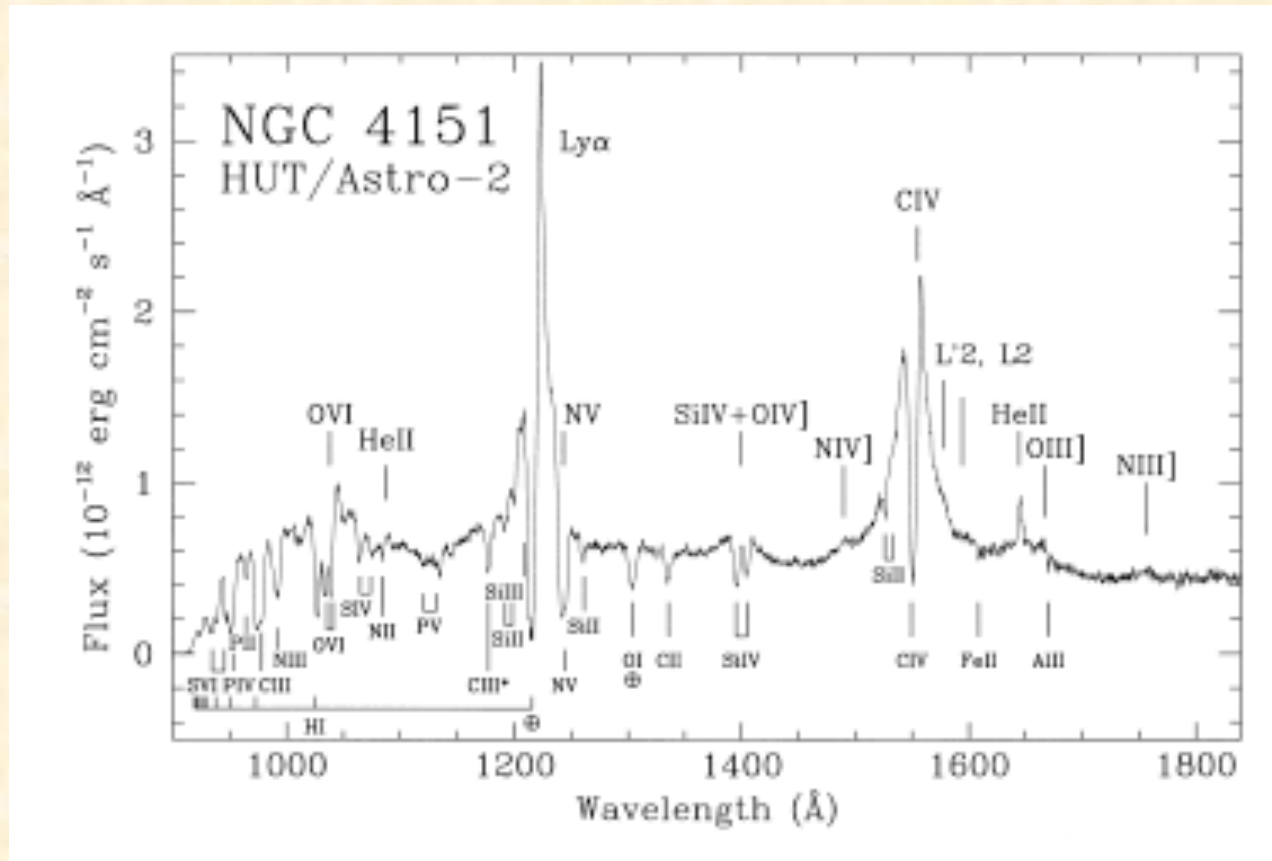
(Hutchings, et al., 2002, AJ, 224, 2543)

- Originally detected in optical spectra of NGC 4151 (Oke & Sargent 1968)
- Blueshifted He I and H I Balmer lines ($n_e > 10^8 \text{ cm}^{-3} \rightarrow$ rare in Seyferts)
- UV absorption in resonance lines much more common ($\sim 60\%$ of Seyferts) (Crenshaw, Kraemer, & George, 2003, ARAA, 41, 117).

Types of UV Absorption Lines - Summary

1. Galactic: Milky Way disk and halo (“high velocity clouds”)
2. Intervening ($z_{\text{abs}} \ll z_{\text{emis}}$)
 - Metal-line systems (“damped Ly α ”): galactic halos and disks
 - “Ly α forest”: IGM clouds (also some O VI, other high-ionization lines)
3. Seyfert “intrinsic” absorption lines
 - Mass outflow: up to -4000 km s^{-1} (probably related to QSO associated)
 - Intrinsic to host galaxy (very narrow, within 300 km s^{-1} of galaxy z)
4. Quasar narrow absorption lines (“NALs”): $\text{FWHM} \leq 300 \text{ km s}^{-1}$
 - “Associated”: mass outflow up to 5000 km s^{-1}
 - “High-velocity NALS”: mass outflow up to $50,000 \text{ km s}^{-1}$
5. Quasar Broad Absorption Lines
 - Hi-BALs: velocity widths $> 2000 \text{ km s}^{-1}$, outflow up to $\sim 0.2c$; high-ionization lines (C IV, N V, etc.)
 - Low-BALs: same as above, plus Mg II and other low-ionization lines
 - Mini-BALs: velocity widths between ~ 500 and 2000 km s^{-1}

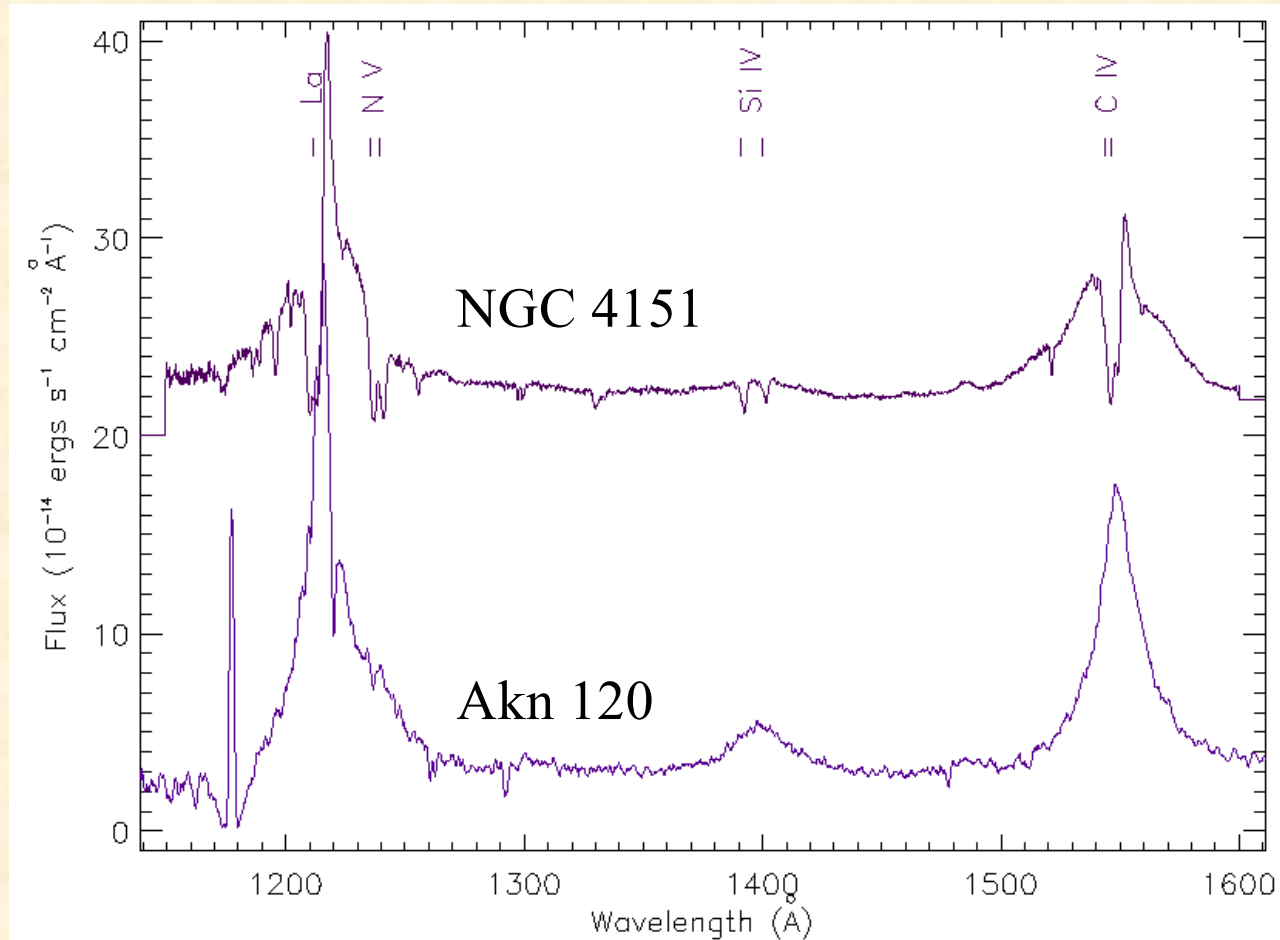
IUE/HUT Observations of Intrinsic UV Absorption



(Kriss et al., 1995, ApJ, 454, L7)

- *IUE* discovered absorption spanning a wide range in ionization (O I to N V)
- *HUT* extended the ionization range to O VI, in the far-UV
- Ulrich (1988) found that 3 - 10% of *IUE* Seyferts have intrinsic absorption

HST Survey of Seyfert Galaxies



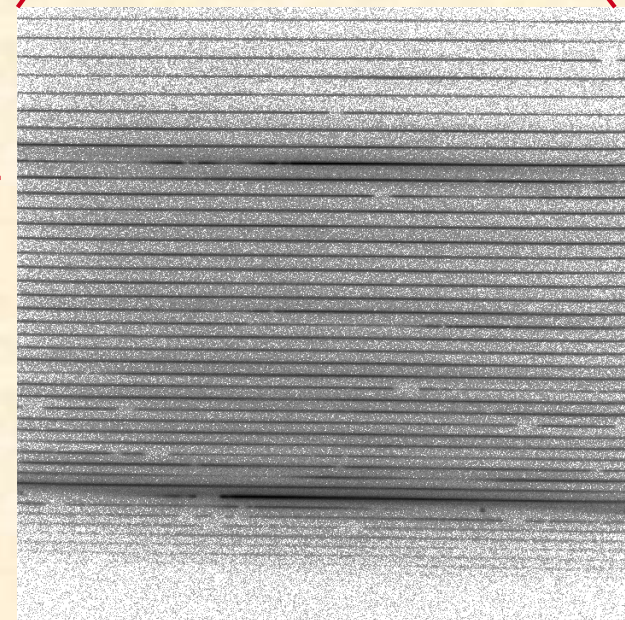
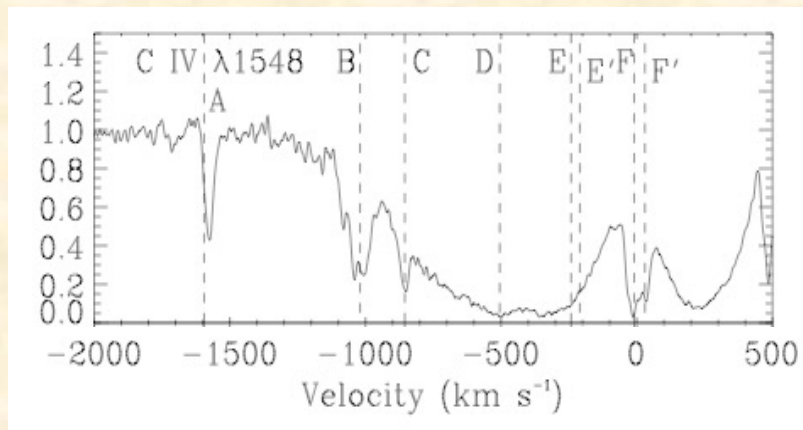
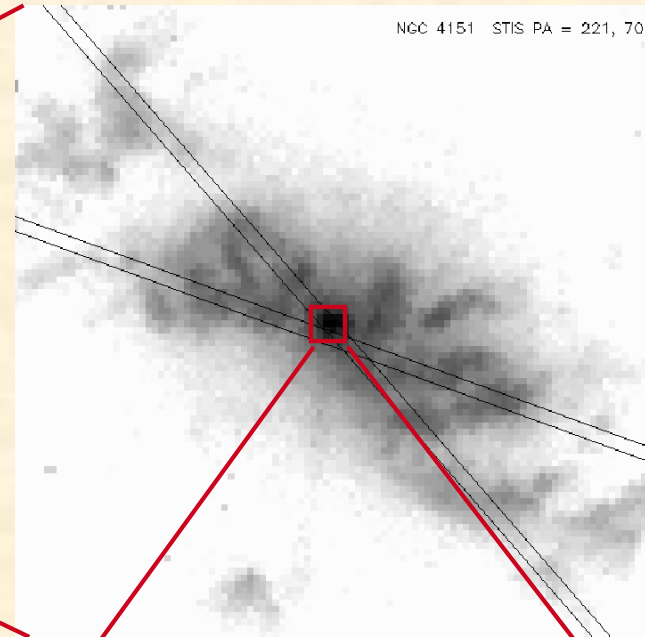
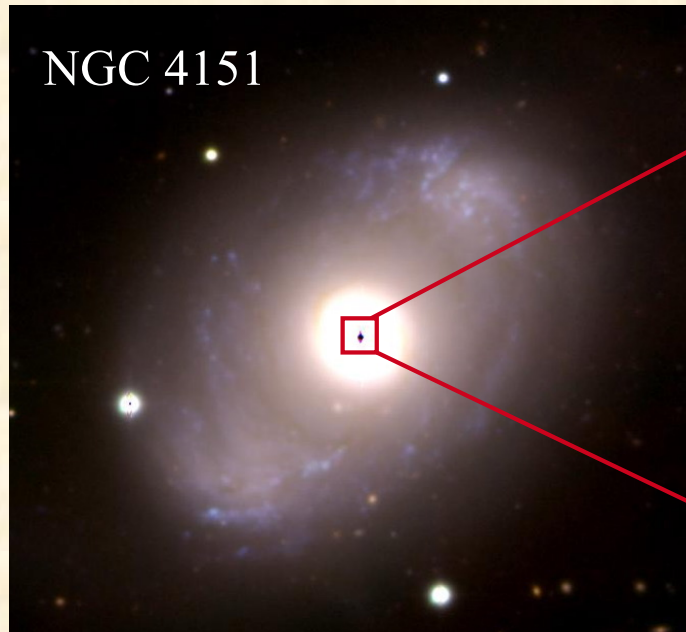
Intrinsic
absorption

No intrinsic
absorption

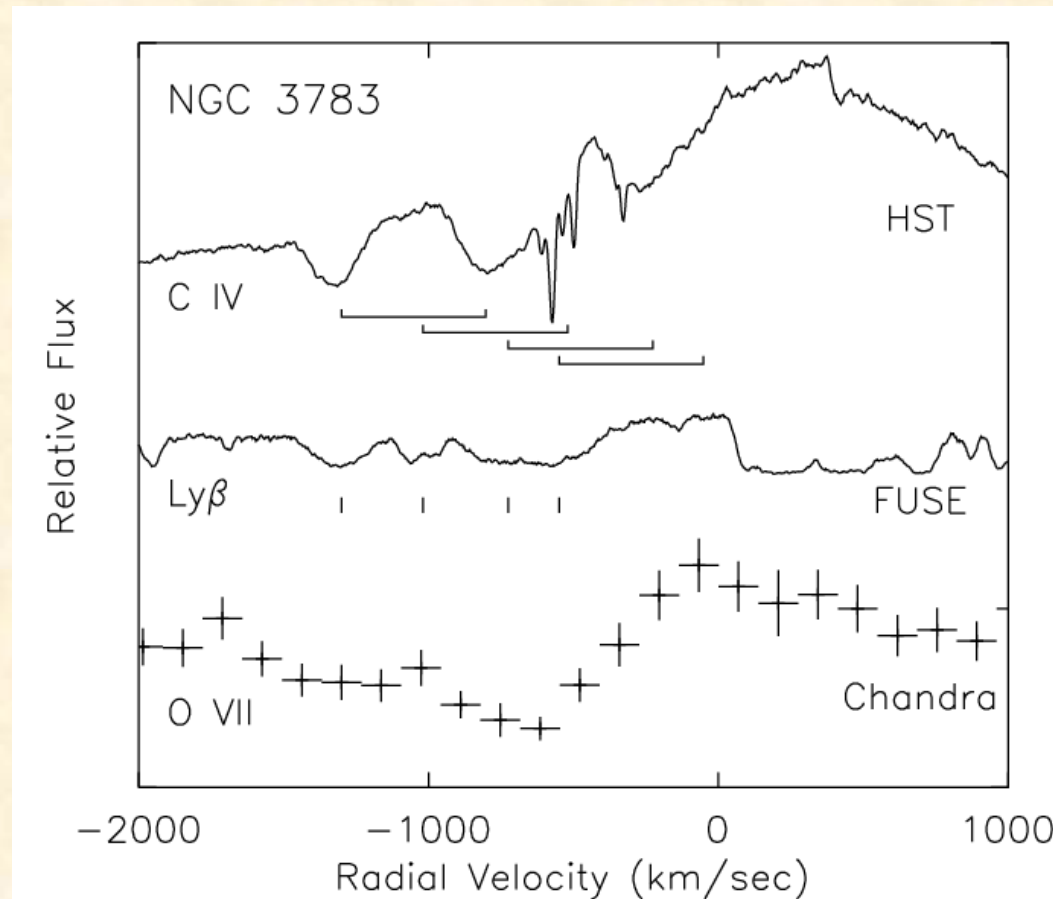
(Crenshaw et al. 1999, ApJ, 516, 750)

- 60% of Seyfert 1 galaxies show intrinsic absorption; those that show UV absorption also show X-ray absorption.
- Global covering of the continuum source and BLR: $C_g = 0.5 - 1.0$
- Most absorbers are highly ionized (C IV, N V); only 10% show Mg II

HST/STIS High-Resolution Spectra



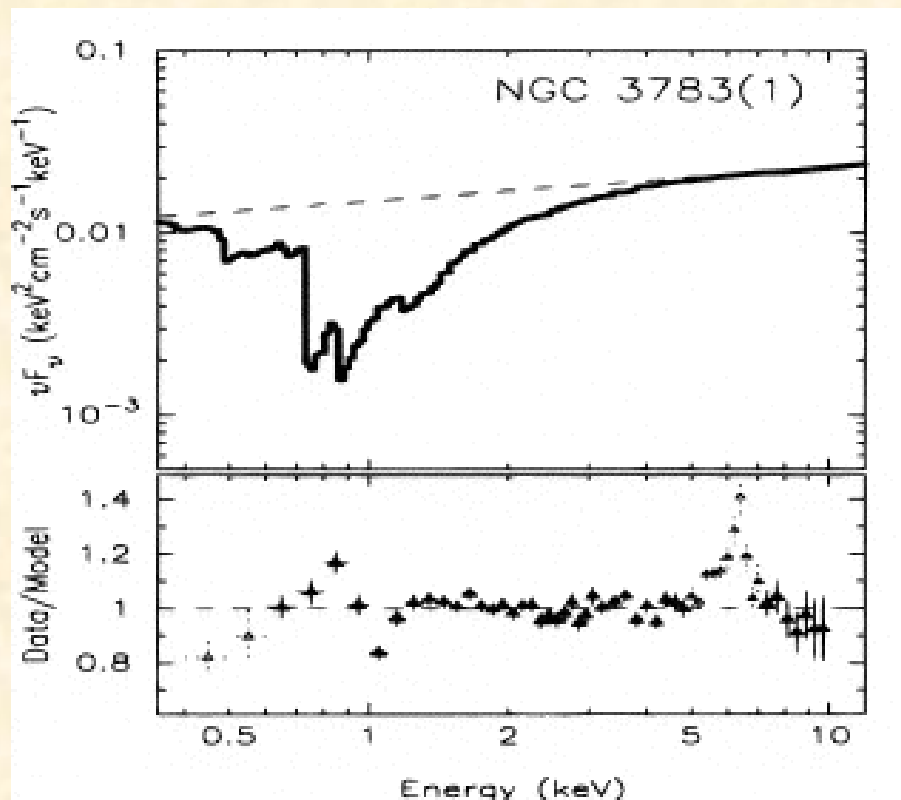
High Resolution Spectra



(Gabel, et al. 2003, ApJ, 583, 178)

- Multiple **outflowing** components detected in UV and far-UV.
- Similar velocity coverage for X-ray absorbers; however X-ray absorbers have higher ionization parameters (U) and column densities (N_H)
- Comparison of UV doublets indicates partial covering of BLR in some cases
- Mass outflow rates can be 10 to 1000x the accretion rates (Crenshaw et al. 2012) 14

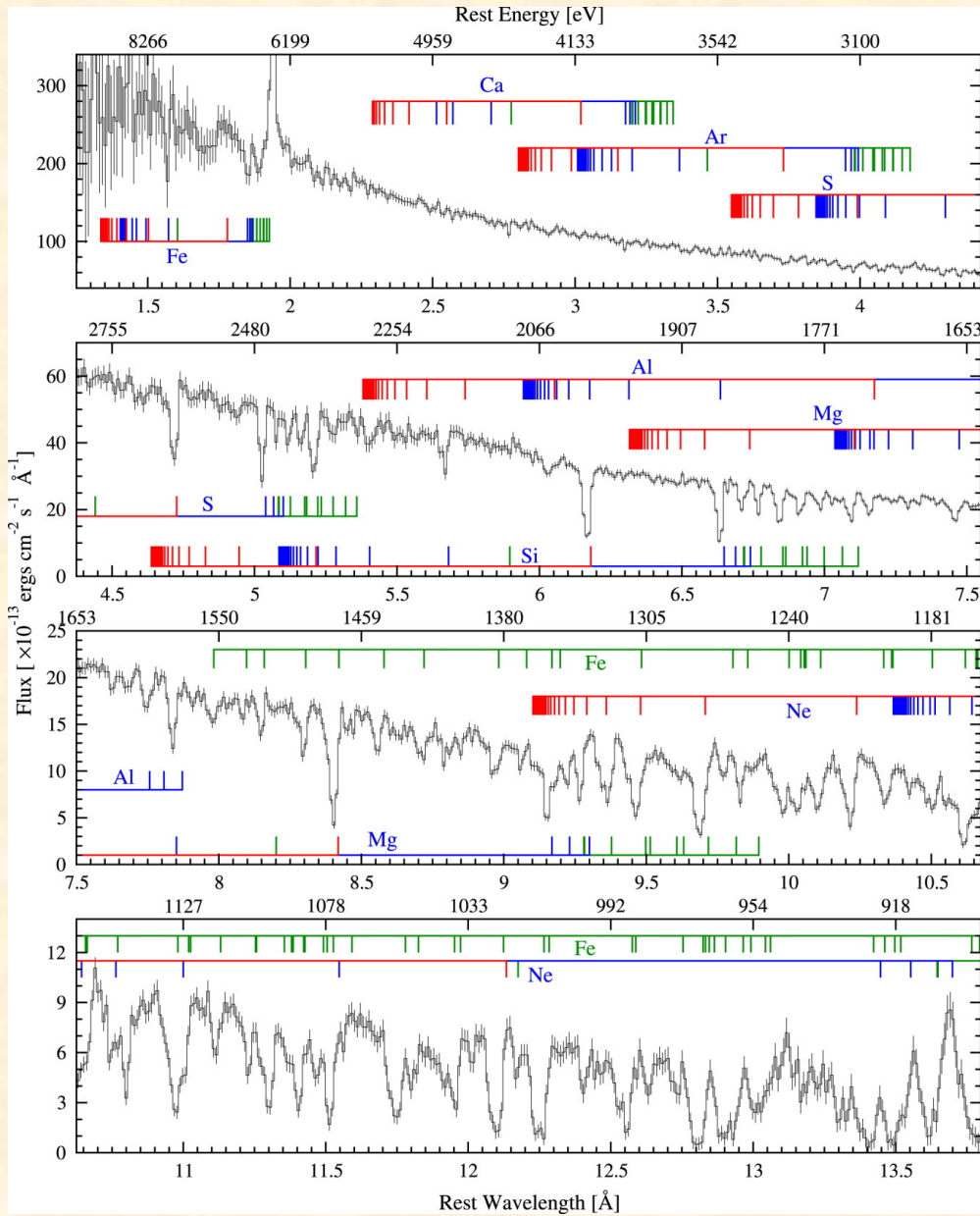
5) X-ray “Warm Absorbers” in Seyferts



(George, et al. 1998, ApJS, 114, 73)

- Absorption by highly-ionized gas first claimed by Halpern (1984)
- Confirmed by *ASCA* detections of O VII and O VIII edges (see above)
- Mathur (1994) claimed a connection between X-ray and UV absorbers
- Blueshifted absorption lines seen by *Chandra* confirmed outflow

Chandra 900 ks Spectrum of NGC 3783



(Kaspi et al. 2002, ApJ, 574, 643)

How do we get more Info? → Variability Monitoring

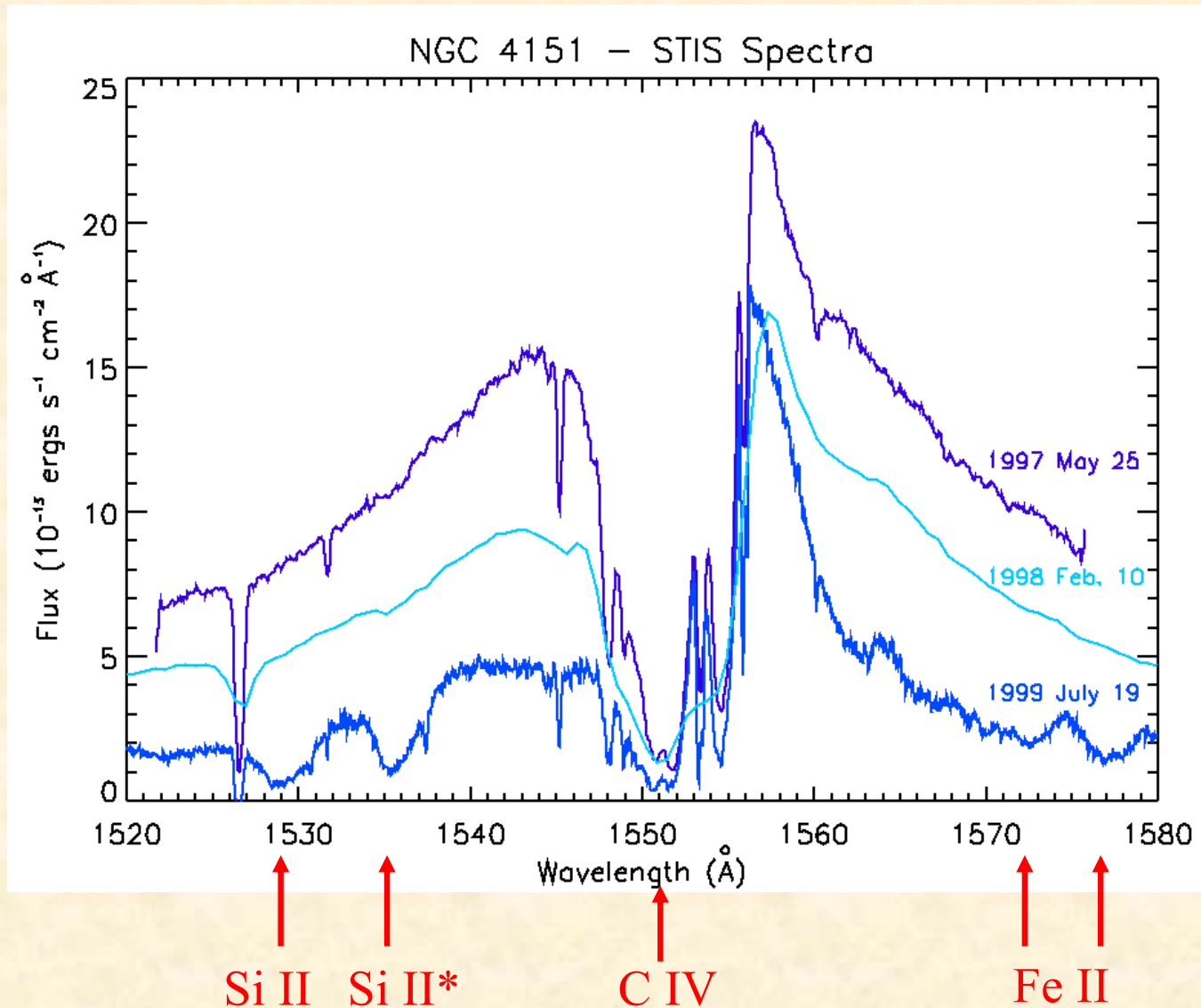
- Nearly all Seyfert 1 galaxies with intrinsic UV absorption show components with variable equivalent widths (EWs)
- Sources of EW (or ionic column density) variations:
 - 1) Variations in the ionizing continuum flux (variable U)
 - 2) Transverse motion of cloud across the BLR + continuum (variable N_{H} or covering factor in the line of sight)
- **Variable ionizing continuum:** can determine density (n_e) and distance from source (r) from time scale of variability (t)

$$n_e \approx \frac{1}{\alpha t_{\text{rec}}} \quad U = \frac{\int_{\nu_0}^{\infty} L_{\nu} / h\nu d\nu}{4\pi r^2 c n_e} \quad (\text{U from photoion. models})$$

- **Transverse motion:** can determine the transverse velocity

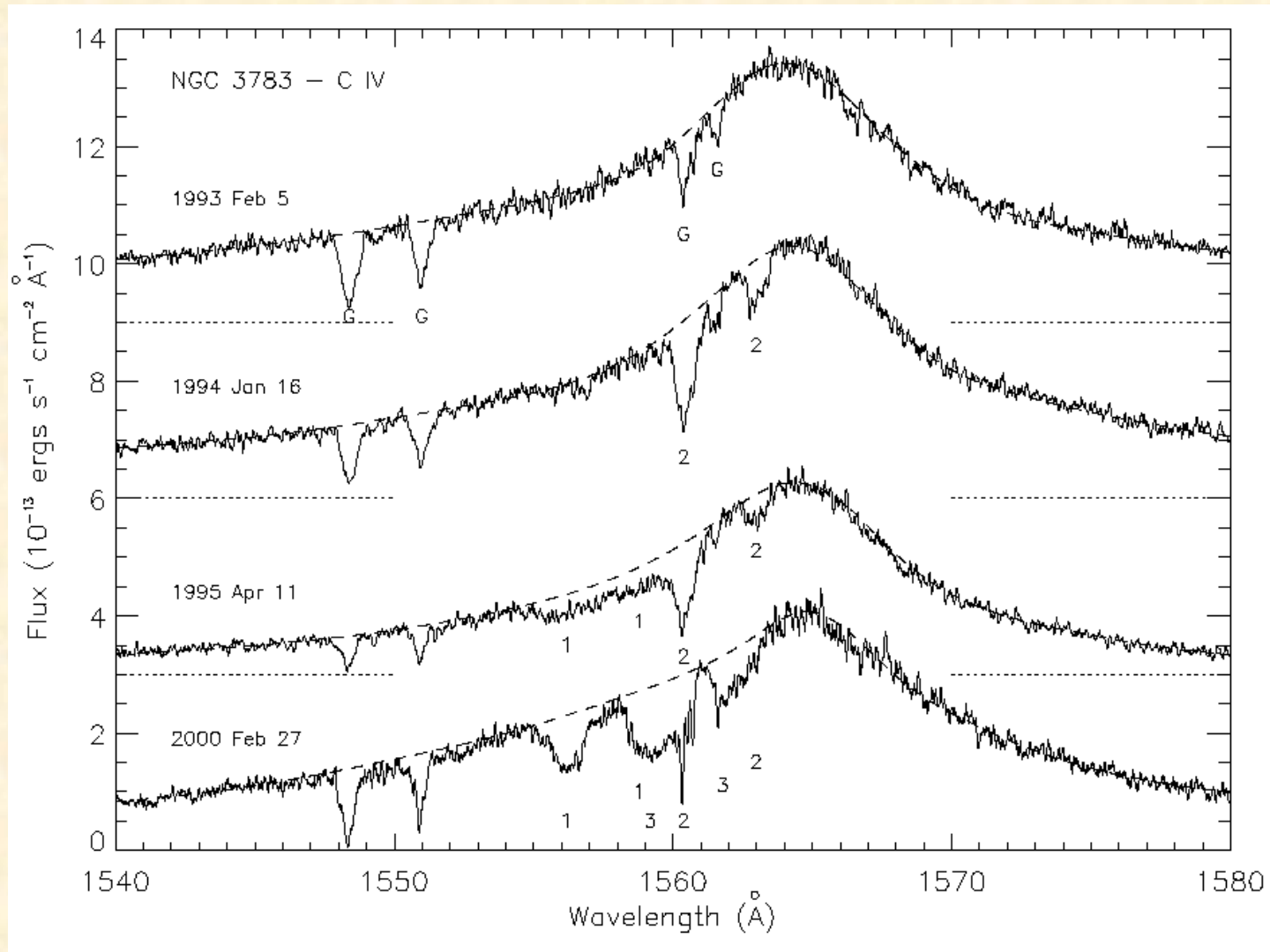
$$v_T = \sqrt{C_{\text{BLR}}} d_{\text{BLR}} / t, \quad \text{where } C_{\text{BLR}} \text{ is the los covering factor}$$

NGC 4151 - Variability in Ionizing Flux



- Low-ionization lines “appear at low continuum \rightarrow variable U

NGC 3783 – Variability due to Transverse Motion



$$\text{Comp. 1 transverse velocity: } v_T = \sqrt{C_{\text{BLR}} d_{\text{BLR}}} / \Delta t \geq 550 \text{ km s}^{-1}$$

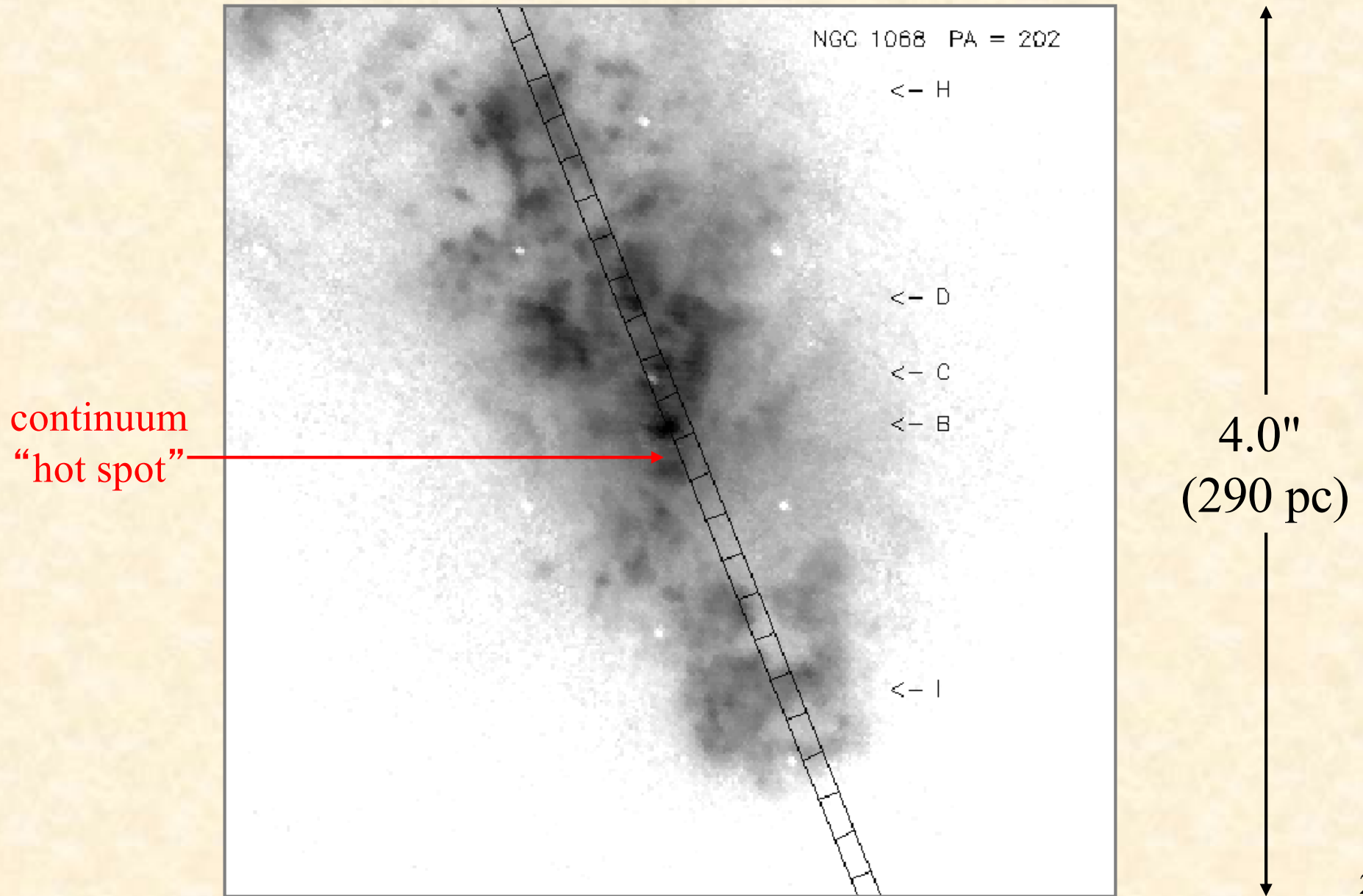
Why are AGN outflows important?

- Quasar outflows have likely:
 - 1) contributed to the heavy-element abundance of the IGM (Hamann & Ferland, 1999, ARA&A, 37, 487)
 - 2) influenced formation of structure in the early Universe (Scannapieco & Peng 2004, ApJ, 608, 62)
 - 3) regulated the growth of supermassive black holes and galactic bulges (Ciotti & Ostriker, 2001, ApJ, 551, 131)
- Seyfert galaxies are the best AGN for probing the machinery of mass outflow in the form of AGN winds.
 - 1) Of all AGN, they have the largest apparent brightness.
 - 2) They are nearby ($z < 0.1$), and offer the best hope of directly resolving the outflowing gas.

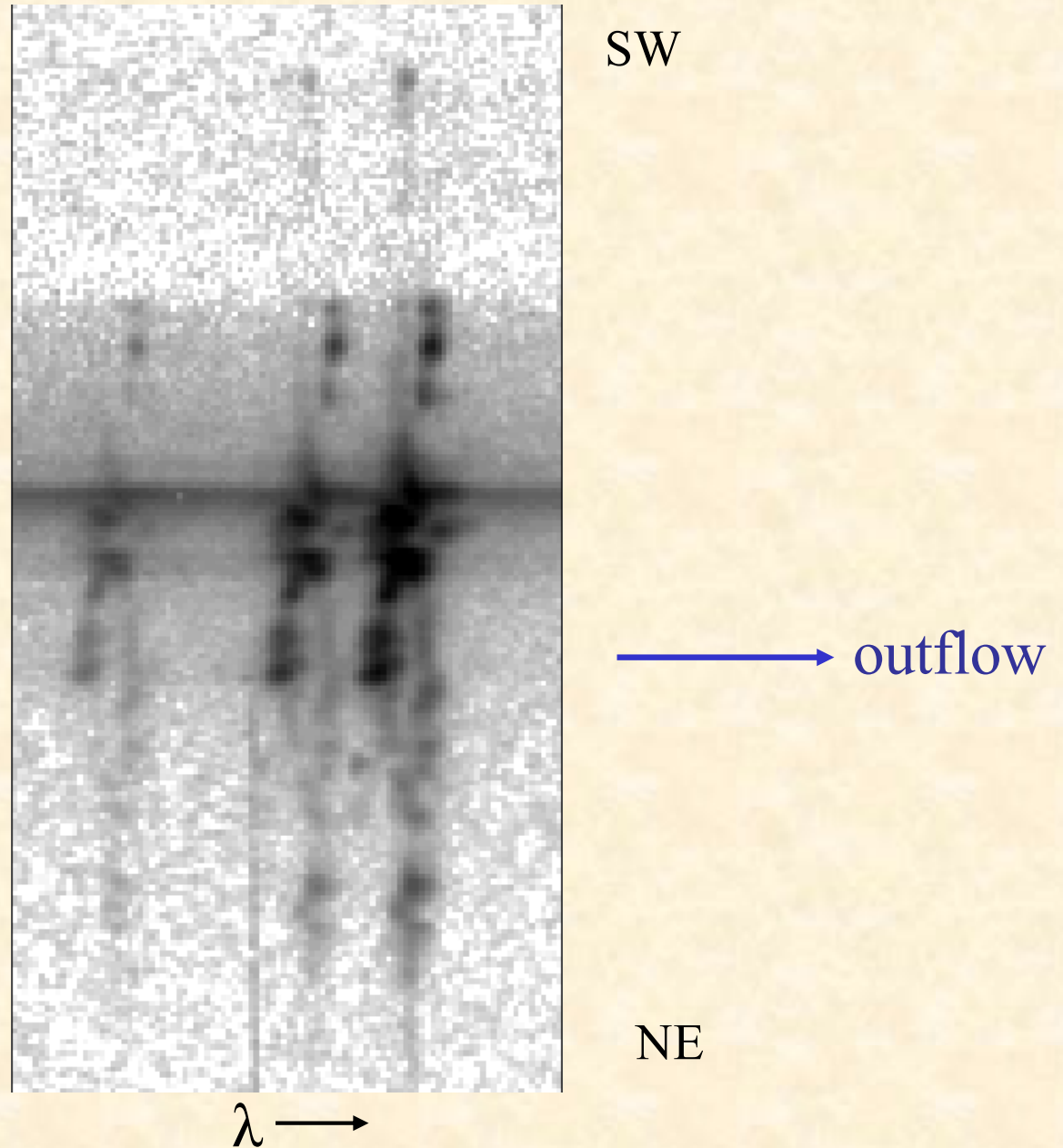
Emission-Line Outflows in the NLR

- Previous ground-based studies have claimed infall, rotation, parabolic orbits, outflow, etc.
- The problem: they relied on spatially integrated line profiles, since the NLR is only a few arcsecs across.
- HST/Space Telescope Imaging Spectrograph has angular resolution $\sim 0.1''$.
- Large ground-based telescopes + adaptive optics (AO) + integral-field units (IFUs) also approach this resolution
→ strong evidence for outflows in the NLR (Crenshaw et al. 2010, ApJ, 708, 419)

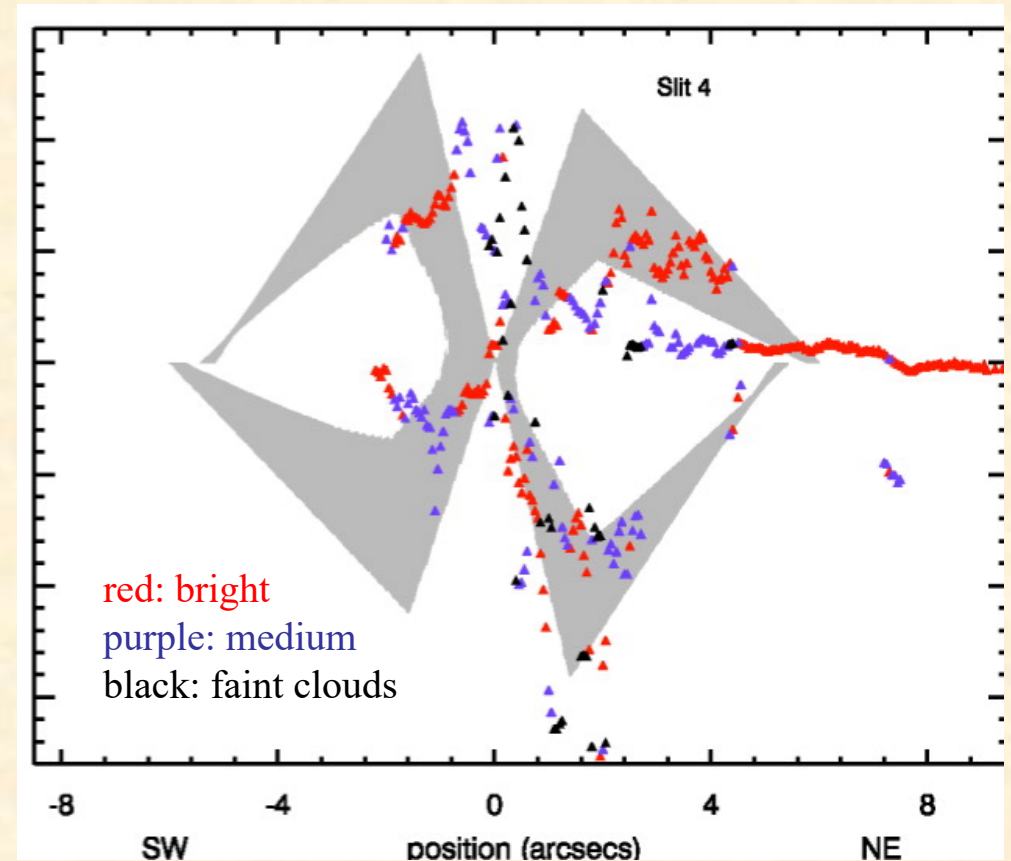
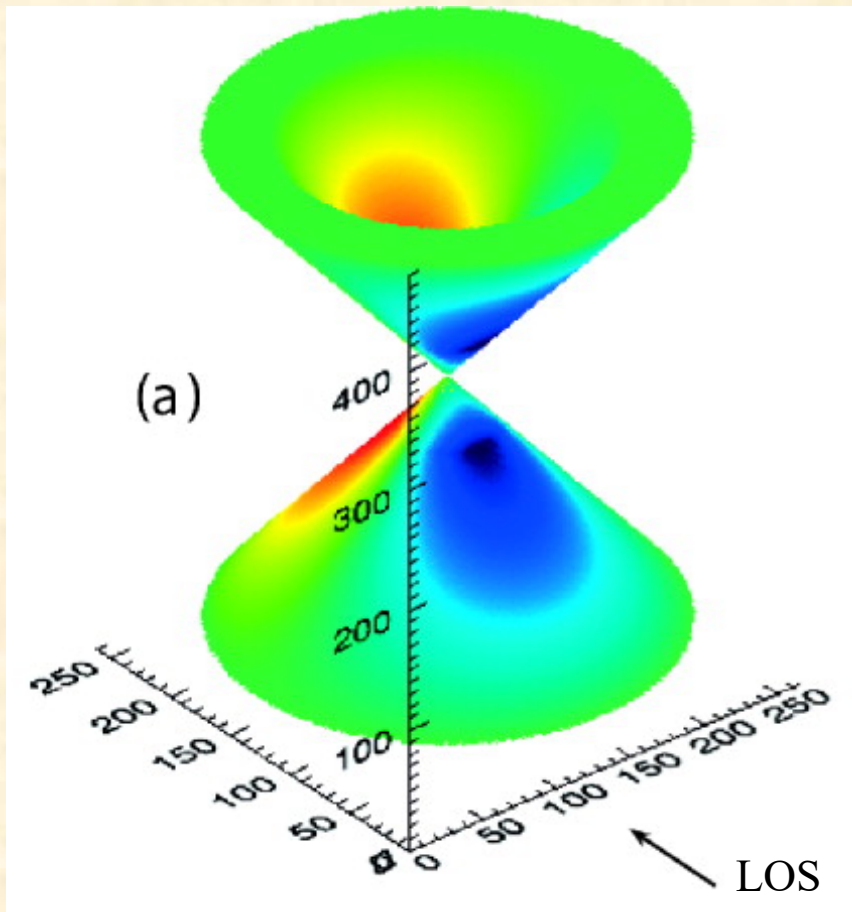
NGC 1068: NLR – [O III] Image



NGC 1068: STIS Long-Slit Spectrum ($H\beta$, [O III])



Biconical Outflow Model for the NLR in NGC 1068

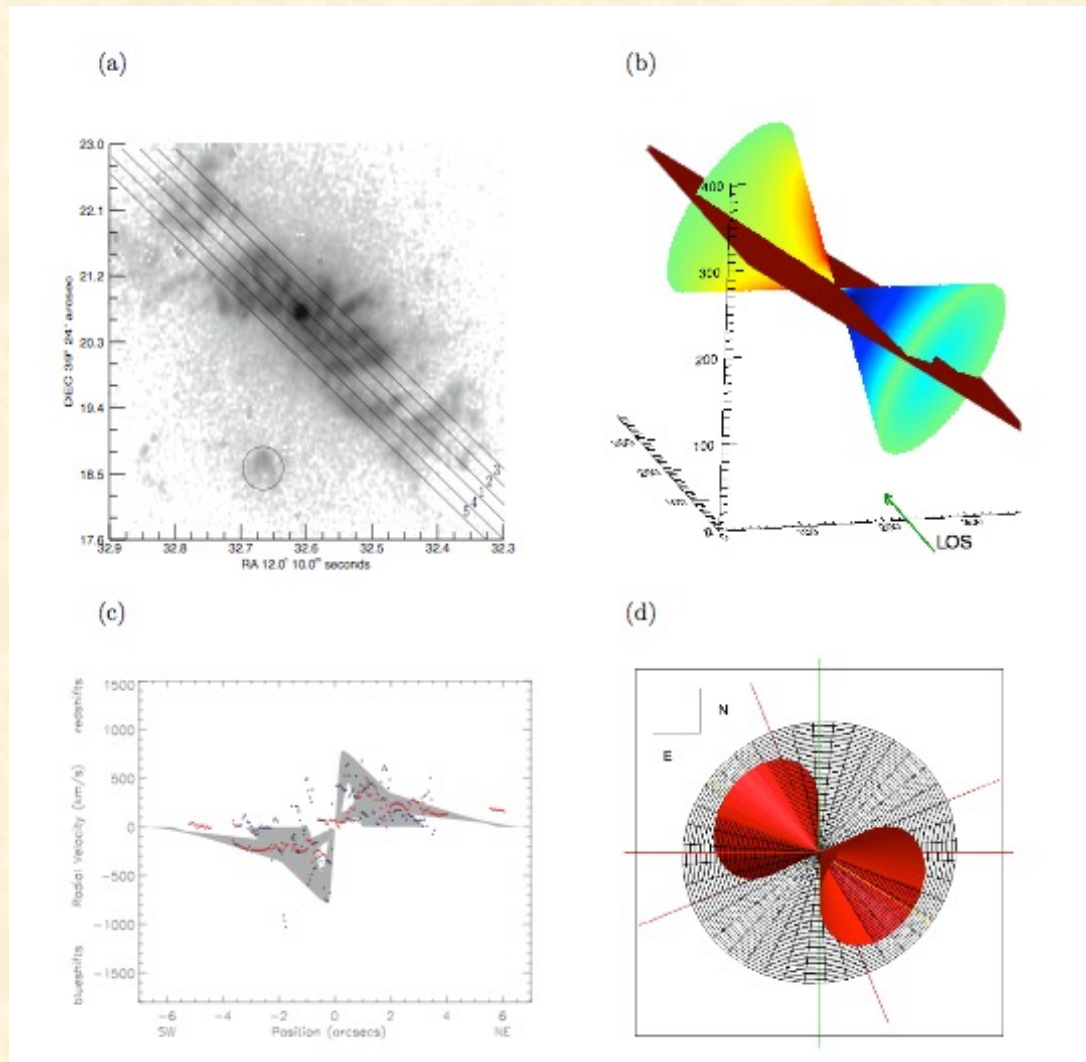


(Das et al. 2006, AJ, 132, 620)

$$\text{incl} = 5^\circ, \theta_{\text{max}} = 40^\circ, \theta_{\text{min}} = 26^\circ, v_{\text{max}} = 1300 \text{ km/sec}, r_t = 137 \text{ pc}$$

- Outflow matches the general trend.
- Radial acceleration followed by deceleration.

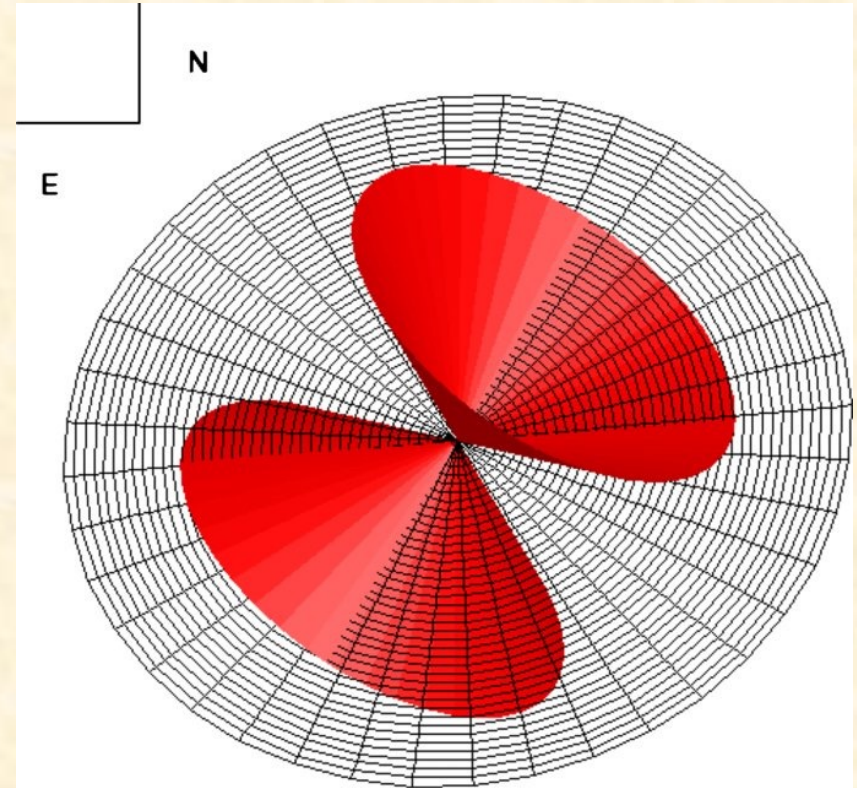
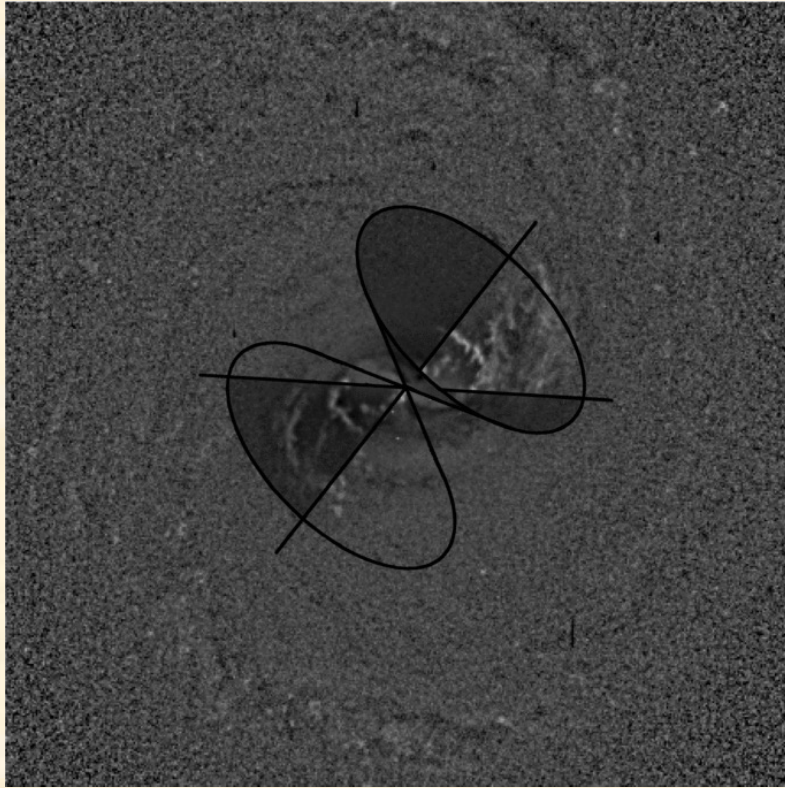
Kinematics of the Narrow-Line Region in NGC 4151



(Das et al. 2005, AJ, 130, 945)

$$\text{incl} = 45^\circ, \theta_{\text{max}} = 33^\circ, \theta_{\text{min}} = 15^\circ, v_{\text{max}} = 800 \text{ km/sec}, r_t = 96 \text{ pc}$$

Mrk 573 – Ionized Spirals in the NLR



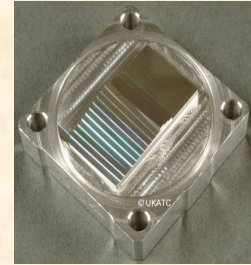
(Fischer et al. 2010, AJ, 140, 577)

- NLR geometry due to intersection between host disk and ionizing bicone.
- Kinematic indicate “in situ” acceleration of gas from the dust spirals.

What is the importance of NLR outflows?

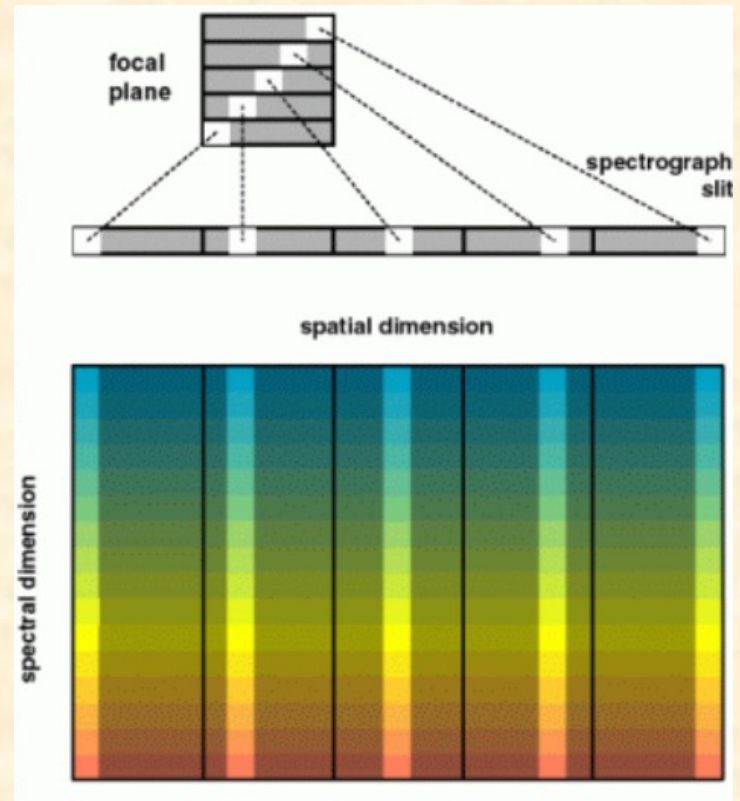
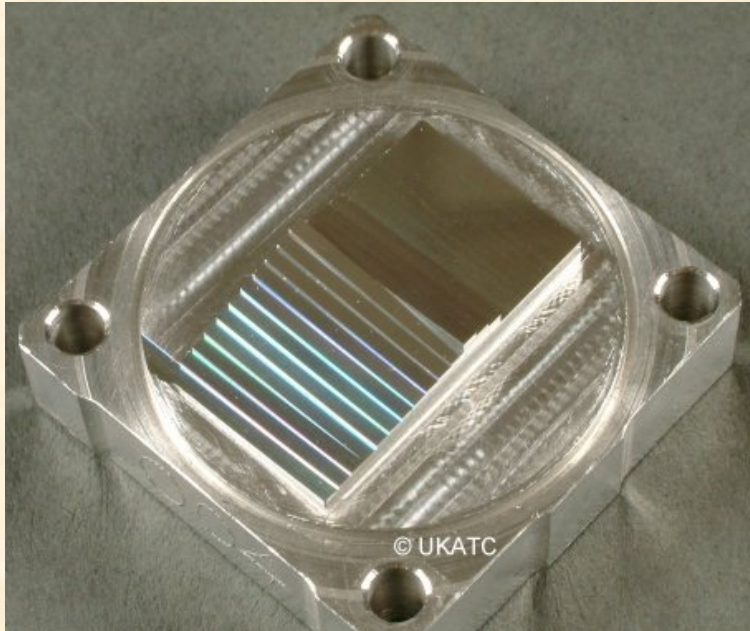
- Provide AGN feedback on scales of hundreds of parsecs
 - may regulate black hole growth, terminate star formation, and explain black-hole mass/bulge correlations
- Provide alternate explanation for double-peaked NLR emission lines (Fischer et al. 2011)
 - Often used to claim double SMBHs in distant merging galaxies
- Kinematic models can determine the *inclination* of the AGN system (bicone, torus, and presumably accretion disk)
 - Investigate how intrinsic properties (SED, BLR velocities, absorber column densities) change with polar angle

NLR Studies: Integral Field Units

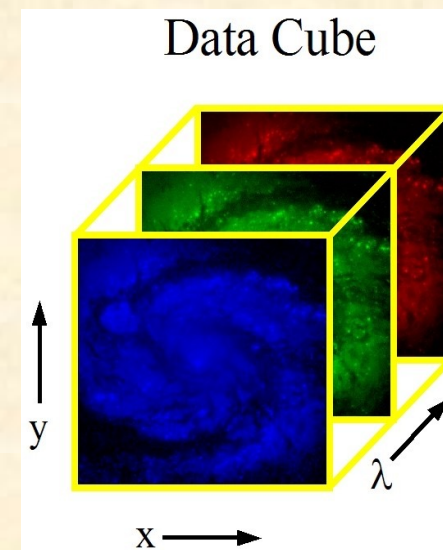
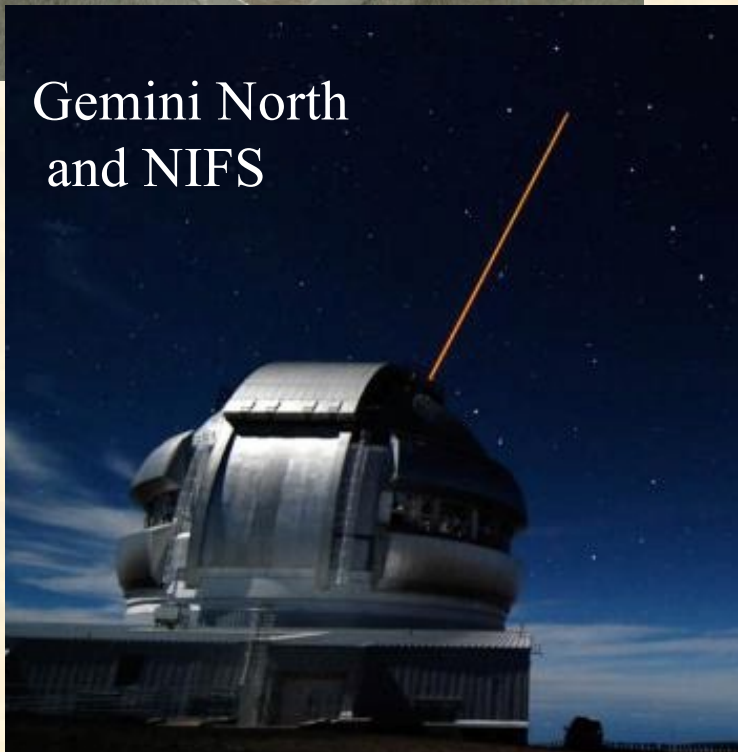


- Spectrum for every position in a field of view
- Three Basic Types
 - Lenslets: microlens array can be tilted around the optical axis so that spectra do not run into each other (allowed length of spectra is small) **Ex) WHT Sauron**
 - Fiber Optics: fibers transfer light to the spectrograph slit (there are gaps between the fibers) **Ex) Gemini GMOS**
 - Image Slicers: instrument mirror segmented into thin vertical slices that are slightly tilted with respect to each other (difficult to fabricate) **Ex) Gemini NIFS**
- Best used with adaptive optics (AO) on large telescopes to give angular resolution of $\sim 0.1''$

Integral Field Unit – Image Slicer



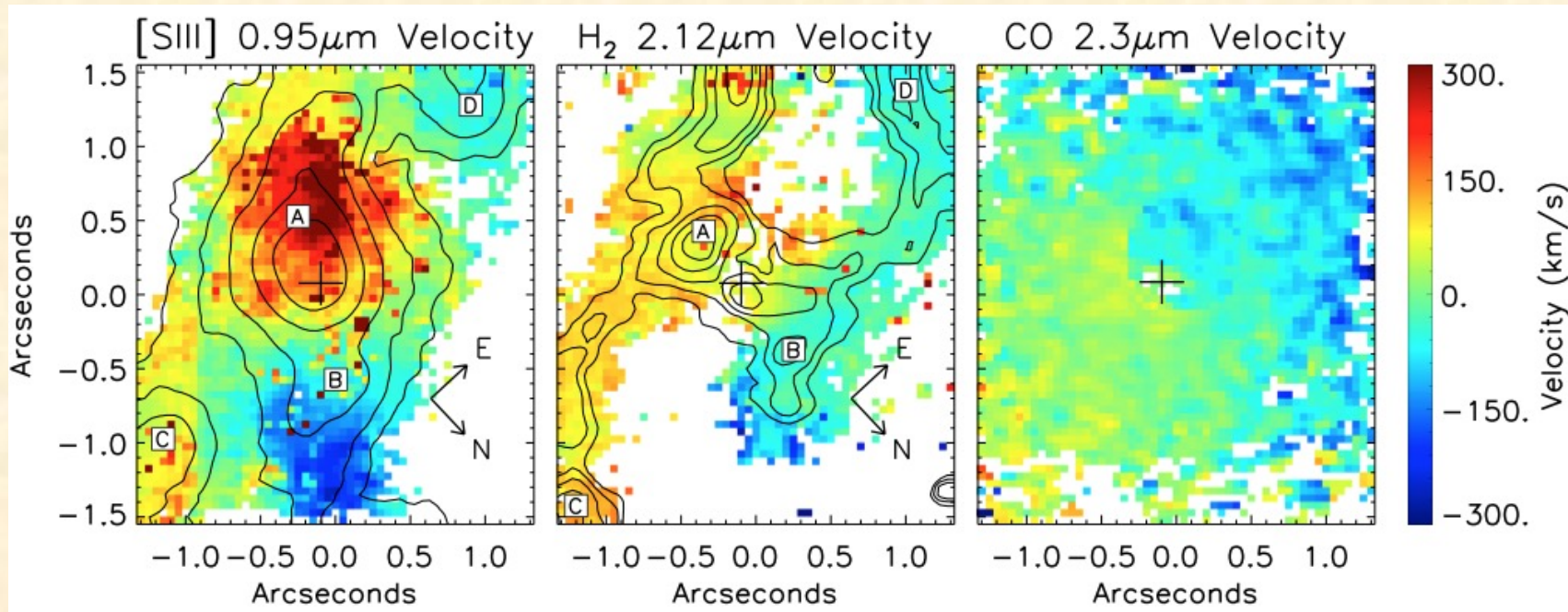
Gemini North
and NIFS



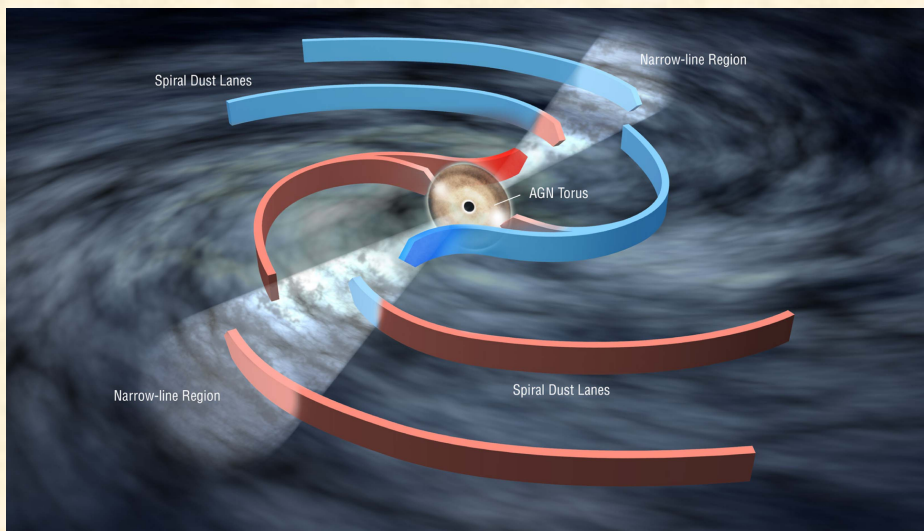
Near-infrared Integral Field Spectrometer (NIFS)

- Only available on Gemini North
- Spectral Resolving Power ~ 5000 over $3'' \times 3''$ at $\sim 0.1''$ angular resolution
- Spectra in **Z** ($0.9 - 1.1\mu\text{m}$), **J** ($1.1 - 1.3\mu\text{m}$), **H** ($1.5 - 1.8\mu\text{m}$), and **K** ($2.0 - 2.4\mu\text{m}$) bands
- Works with adaptive optics system ALTAIR using natural or laser guide stars
- For AGN, access to:
 - [S III] emission in Z band to map ionized gas in the NLR
 - H_2 emission lines in K band to map warm molecular gas
 - CO bandheads and other stellar features in H and K bands to map stellar velocities and dispersions for determining black hole masses.

Gemini NIFS Observations of Mrk 573



(Mrk 573: Fischer+ 2017, ApJ, 834, 30)



- Gas in dusty molecular spirals is ionized and radiatively driven outward
- Mass outflow rate peaks at $\sim 3 M_{\text{Sun}}/\text{yr}$ (Revalski et al. 2018, 2021).

Dynamical Forces in the Narrow-Line Region (NLR)

Radiative acceleration: $a_r(r) = \frac{L\sigma_T\mathcal{M}}{4\pi r^2 c\mu m_p}$ ($\mu = \text{mean atomic mass} = 1.4$, addition to Das+2006)

Gravitational deceleration: $a_g(r) = -\frac{GM(r)}{r^2}$ ($\mathcal{M} = \text{force multiplier compared to Thomson scattering}$
 $(M(r) = \text{enclosed mass})$)

Total acceleration: $a(r) = a_r(r) + a_g(r)$

$$a(r) = \frac{dv}{dt} = \frac{dv}{dr} \frac{dr}{dt} = \frac{dv}{dr} v$$

$$\int_0^v v dv = \int_{r_1}^r [a_r(r) + a_g(r)] dr$$

$$v = \sqrt{2 \int_{r_1}^r [a_r(r) + a_g(r)] dr} \quad v = \sqrt{2 \int_{r_1}^r \left[\frac{L\sigma_T\mathcal{M}}{4\pi r^2 c\mu m_p} - \frac{GM(r)}{r^2} \right] dr}$$

Velocity Profile:

$$v(r) = \sqrt{\int_{r_1}^r \left[4885 \frac{L_{44}\mathcal{M}}{r^2} - 8.6 \times 10^{-3} \frac{M(r)}{r^2} \right] dr} \quad v \left(\text{km s}^{-1} \right); r(\text{pc}); L_{44} (10^{44} \text{ erg s}^{-1}); M(M_{\odot})_{32}$$

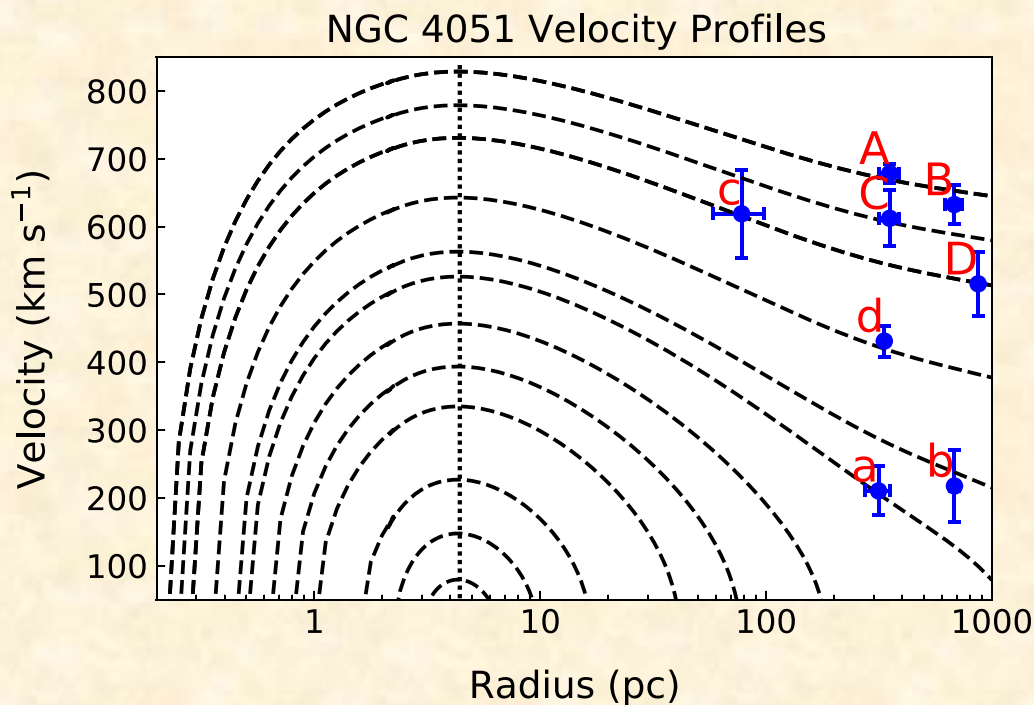
Launch radius (r_1) – match calculated and observed $v(r)$ for a NLR knot to get r_1 (the only unknown):

$$v(r) = \sqrt{\int_{r_1}^r \left[4885 \frac{L_{44} M}{r^2} - 8.6 \times 10^{-3} \frac{M(r)}{r^2} \right] dr} \quad (r - r_1 = \text{distance traveled}, t = \sum \frac{\Delta r}{v} = \text{time traveled})$$

Model velocity turnover (max launch radius): $a_r(r_m) = a_g(r_m)$ $r_m = r_1$ (max), independent of other r_1

Note: The above assumes:

- 1) purely radial motion - gas at launch point is not rotating, so no azimuthal velocity
- 2) spherical symmetry (e.g., bulge dominates near core) or axisymmetry (e.g. radial motion in disk)

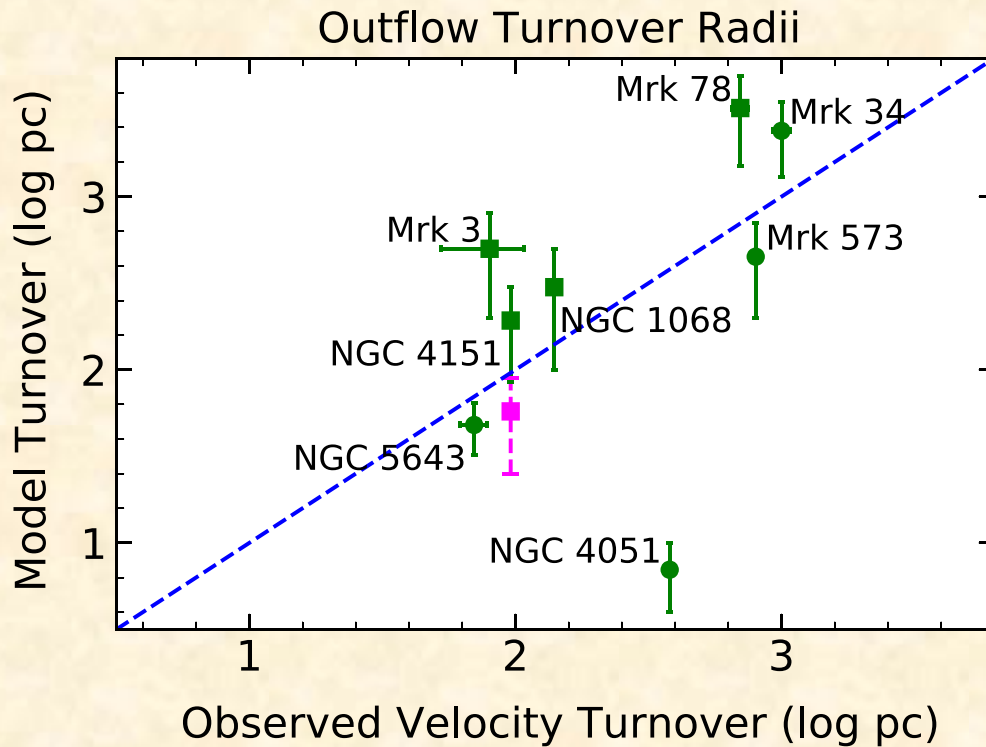


(Meena+ 2021, 916, 31)

NGC 4051:

- Clouds launched between 0.2 – 4 pc.
- Max launch radius \approx 4 pc, all velocities turn over at this point
- Clouds can travel up to \sim 1 kpc.

Comparison with Observations



(Meena+2023, ApJ, 943, 98)

- Increasing luminosity to the right.
- Correlation indicates radiative driving + grav. decel. control NLR dynamics.
- Any acceleration of gas or increasing \dot{M}_{out} beyond r_{mod} would indicate additional forces.
- What value of \mathcal{M} would get the best match (excluding NGC 4151)? – about 500
- Does this relation hold for low luminosity? (may not be able to resolve turnover point)
- LINERs (with $L/L_E < 10^{-3}$) should not be able to radiatively launch outflows.